



Published in final edited form as:

Medchemcomm. 2015 June 1; 6(6): 1065–1068. doi:10.1039/C5MD00148J.

## Synthesis and evaluation of [<sup>11</sup>C]PBD150, a radiolabeled glutaminyl cyclase inhibitor for the potential detection of Alzheimer's disease prior to amyloid β aggregation

Allen F. Brooks<sup>a</sup>, Isaac M. Jackson<sup>a</sup>, Xia Shao<sup>a</sup>, George W. Kropog<sup>a</sup>, Phillip Sherman<sup>a</sup>, Carole A. Quesada<sup>a</sup>, and Peter J.H. Scott<sup>a,b,\*</sup>

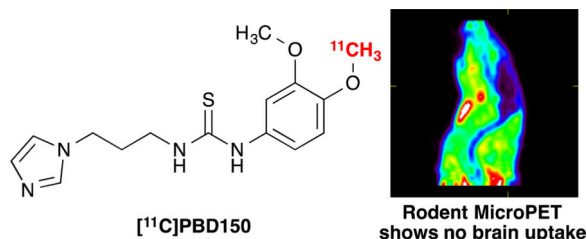
<sup>a</sup>Division of Nuclear Medicine, Department of Radiology, The University of Michigan Medical School, 2276 Medical Science I Building, Ann Arbor, Michigan 48109, USA

<sup>b</sup>The Interdepartmental Program in Medicinal Chemistry, The University of Michigan, 428 Church St., Ann Arbor, Michigan 48109, USA

### Abstract

The phenol of 1-(3-(1H-imidazol-1-yl)propyl)-3-(4-hydroxy-3-methoxyphenyl)thiourea was selectively carbon-11 labelled to generate [<sup>11</sup>C]PBD150 in 7.3% yield from [<sup>11</sup>C]methyl triflate (non-decay corrected; radiochemical purity 95%, specific activity = 5.7 Ci/μmol, n=5). Evaluation of [<sup>11</sup>C]PBD150 by small animal PET imaging (mouse and rat) determined it does not permeate the blood brain barrier, indicating previously described therapeutic effect in transgenic mice was likely not the result of inhibiting central nervous system glutaminyl cyclase.

### Abstract



Glutaminyl cyclase (QC) is an enzyme primarily expressed in the brain with a large amount of expression in the hippocampus and cortex. QC is responsible for the formation of pyroglutamate (pGlu) at the N-terminus of several neuropeptides including amyloid β (Aβ).<sup>1</sup> This modification is important for the biological function of those neuropeptides, and importantly the pGlu modification stabilizes the peptide against proteolytic decomposition.<sup>2</sup> Changes in QC expression between Alzheimer's disease (AD) patients and healthy control subjects have not been fully analyzed and absolutely quantified yet. However, a post-

mortem study of human neocortical brain samples found AD patients had upregulated levels of QC mRNA compared to patients without dementia, while immunohistochemistry suggests 20–30% higher expression of QC in all cortical layers of AD patients compared to controls.<sup>3</sup> This increase in QC leads to the formation of pGlu-A $\beta$  peptides that are more neurotoxic and resistant to removal than normal A $\beta$ . They act similar to a prion, providing a template for misfolding and as a seed for aggregation<sup>4</sup> with unmodified A $\beta$ .<sup>5</sup> The pGlu modified variants of A $\beta$  have been shown to be present in the plaques of AD brains by several different analytical methods: immunohistochemistry and immunocytochemistry for distinct A $\beta$  species,<sup>6, 7</sup> mass spectrometry of plaques,<sup>7, 8</sup> incubation with pGlu aminopeptidase to verify the presence of pGlu modification,<sup>9</sup> and a sandwich enzyme-linked immunosorbent assay to quantify amount of pGlu modified A $\beta$ .<sup>10</sup> The prion like role played by pGlu-A $\beta$  species in the formation of aggregates in AD that are the result of upregulated QC lead us to hypothesize that a QC inhibitor amenable to radiolabeling would provide a means to detect AD by positron emission tomography (PET) imaging prior to the accumulation of senile plaques.

Many inhibitors of QC have been prepared and screened *in vitro*.<sup>11–14</sup> Radiolabeled examples have been claimed in a recent patent;<sup>15</sup> however, no QC radiotracers have been reported in the literature to date. Interestingly, PBD150 (shown in Figure 1),<sup>11</sup> was not covered in the patent despite having good affinity for the enzyme ( $K_i = 60$  nM for human QC and  $K_i = 173$  nM for murine QC) and being the only agent thus far to have been demonstrated *in vitro* and *in vivo* to reduce the formation of A $\beta$  aggregates.<sup>3a, 11</sup> Radiolabeling PBD150 by methylation with [<sup>11</sup>C]MeOTf or [<sup>11</sup>C]MeI through a phenol precursor is not straightforward as PBD150 contains a thiourea, which can readily undergo methylation instead,<sup>16</sup> making an undesired alternate product.<sup>17</sup> In an example pertinent to PET radiochemistry, Gilissen and co-workers had problems introducing ethyl tosylate groups into methylthioureas for subsequent <sup>18</sup>F-fluorination, obtaining unwanted cyclized by-products instead.<sup>18</sup> To circumvent this issue, the investigators first generated 2-[<sup>18</sup>F]fluoroethylamine, and then introduced the thiourea functionality. Despite these issues, as PBD150 has shown a therapeutic effect when administered orally to transgenic mice,<sup>3a</sup> we resolved to develop a method to carbon-11 label a phenol in the presence of a thiourea so that we could evaluate [<sup>11</sup>C]PBD150 as a PET agent for the detection of AD prior to senile plaque burden.

To radiolabel PBD150 the desmethyl precursor, 1-(3-(1H-imidazol-1-yl)propyl)-3-(4-hydroxy-3-methoxyphenyl)thiourea (**5**), was prepared in 4 steps. The synthesis of the desmethyl precursor, as shown in Scheme 1, was accomplished by acylation of the hydroxyl of 4-nitroguaiacol and subsequent reduction of the nitro of intermediate **2** to give aniline **3**.<sup>19</sup> The aniline was then converted to thioisocyanate **4** with thiophosgene. The product was used directly in the next reaction with 1-(3-aminopropyl)imidazole to form thiourea **5** in 41% yield from **3**. The synthesis of desmethyl precursor (**5**) was completed in 4 steps and an overall yield of 28% from **1**. To confirm the identity of the radiotracer, it was also necessary to synthesize unlabelled reference standards. Authentic PBD150 was synthesized as previously described.<sup>11</sup> Alternate methylation product **6** was also prepared in 11% yield by treating **5** with MeI. Baseline separation of PBD150 and alternate product **6** was readily

achievable by 2 different analytical HPLC methods (see ESI † for representative HPLC traces).

Initial attempts to radiolabel PBD150 by [ $^{11}\text{C}$ ]methylation were investigated using tetrabutylammonium hydroxide (TBA-OH) as a base (Table 1). No product was observed with the preformed tetrabutylammonium phenoxide of **5** using either typical reactor set up with DMF as a solvent in a TRACERLab FX<sub>C-Pro</sub> (Entries 1 and 2) or ethanolic loop chemistry<sup>20</sup> (Entry 3) with either [ $^{11}\text{C}$ ]MeOTf or [ $^{11}\text{C}$ ]MeI. In addition, the subsequent HPLC-UV analysis showed that no precursor remained in these reactions. Based on those results, we decided that a non-nucleophilic base could be required to avoid the decomposition of the precursor. We therefore attempted carbon-11 labelling with NaH using [ $^{11}\text{C}$ ]MeI (Entry 4) or [ $^{11}\text{C}$ ]MeOTf (Entry 5). These conditions resulted in predominantly alternate radiolabelled product **6**, confirmed by comparison of the radio-HPLC with the known retention times of the 2 reference standards (see ESI). The use of a non-nucleophilic base had avoided precursor decomposition but NaH favoured the alternate methylation product [ $^{11}\text{C}$ ]**6**, so we next investigated the use of  $\text{K}_2\text{CO}_3$ , another non-nucleophilic base that has a lower conjugate pKa. Initial attempts using standard conditions ([ $^{11}\text{C}$ ]MeOTf in 3-pentanone, Entry 6) proved ineffective as precursor **5** was insoluble. Ultimately, treatment of the precursor in DMF with 10  $\mu\text{L}$  of a satd.  $\text{K}_2\text{CO}_3$  solution dried over  $\text{Na}_2\text{SO}_4$  prior to labelling with [ $^{11}\text{C}$ ]MeOTf in a reactor (Entry 7) was found to be the best method for generating [ $^{11}\text{C}$ ]PBD150. These conditions were based upon institutional knowledge for radiolabeling phenols (unpublished results), and the use of the more efficient methylating agent is essential. Use of [ $^{11}\text{C}$ ]MeI in the presence of  $\text{K}_2\text{CO}_3$  also favours generation of [ $^{11}\text{C}$ ]PBD150 over [ $^{11}\text{C}$ ]**6**, but in low yield (Entry 8).

The radiolabeling of [ $^{11}\text{C}$ ]PBD150 with [ $^{11}\text{C}$ ]MeOTf using the optimum conditions was then automated in a TRACERLab FX<sub>C-Pro</sub> system. The product was purified by reverse phase HPLC and the ethanolic buffer with product (2 mL) was added to saline (8 mL) to prepare the dose for injection. The synthesis (Scheme 2) resulted in 66.1 mCi of formulated product (7.3% yield from [ $^{11}\text{C}$ ]MeOTf, non-decay corrected; radiochemical purity 95%, specific activity = 5.7 Ci/ $\mu\text{mol}$ , n=5). The doses produced were determined by standard quality control techniques (see ESI) to be appropriate for preclinical studies.

The imaging capability of [ $^{11}\text{C}$ ]PBD150 was investigated through small animal PET imaging with Sprague Dawley rats (n = 2; Figure 2 and ESI). [ $^{11}\text{C}$ ]PBD150 was administered *i.v. via* tail vein injection and dynamic PET scans were acquired for 60 min. post-injection of the radiotracer. Analysis of summed frame images showed no brain uptake and early frames showed no first pass uptake in the brain. The fact that PBD150 had previously demonstrated a therapeutic effect on AD progression in transgenic mice made the lack of blood-brain barrier (BBB) permeability surprising.<sup>3a</sup> To investigate if efflux by P-glycoprotein (Pgp) transporter is an issue with PBD150 (given previous examples observed<sup>21, 22</sup>) cyclosporin A blocking experiments were performed. Animals were treated with cyclosporin A (50 mg/kg) 60 min prior to injection of [ $^{11}\text{C}$ ]PBD150. The imaging data obtained showed no brain uptake as before with baseline scan data. In the work with transgenic mice, PBD150 had been administered orally in the food of the mice for several months.<sup>3a</sup> To examine if brain uptake was facilitated by a higher concentration of PBD150

in the blood, an experiment was conducted where [ $^{11}\text{C}$ ]PBD150 was co-administered, *via* tail vein injection, with an equivalent amount of unlabelled PBD150 to the oral dose reported previously (12 mg total; ~37 mg/kg).<sup>3a</sup> The PET imaging data again showed no brain uptake (Figure 2A), comparable to previous experiments. As the therapeutic studies were conducted in mice,<sup>3a</sup> we also repeated imaging in a female CD-1 mouse to investigate any differences in brain uptake between species. However, there was also no brain uptake of the radiotracer in the mouse brain (see ESI for rat and mouse imaging data), suggesting that the poor brain uptake is not due to a species difference.

For each experiment a region of interest was drawn around the brain and standardized uptake values (SUV) were calculated and charted versus time. The analysis showed no difference between the baseline, cyclosporin A treatment and co-administered experiments (Figure 2B). To investigate whether the imaging results were due to metabolic instability, metabolism of PBD150 was examined by incubation with rat liver microsomes. The LC-MS/MS data analysis at microsome incubation time points out to 60 min (the length of the rodent PET imaging experiments) demonstrated the molecule had a half-life >60 min, with 78% of authentic PBD150 remaining at 60 min, indicating that the lack of brain uptake is likely not due to rapid metabolism of the radiotracer.

In summary, a method for the carbon-11 methylation of a phenol in the presence of thiourea has been developed and applied to the synthesis of [ $^{11}\text{C}$ ]PBD150: a QC inhibitor demonstrated *in vitro* and *in vivo* to decrease the formation of pGlu-A $\beta$ . Preclinical rodent PET imaging experiments with [ $^{11}\text{C}$ ]PBD150 revealed a lack of brain uptake. Further experiments demonstrated that the lack of brain uptake is not due to metabolism, and nor is it due to efflux by Pgp. The reasons for the lack of BBB permeability are unclear at this time, but could simply be due to the polarity of the compound. Nevertheless, this work does suggest that the therapeutic effect observed in transgenic mice in prior literature was not due to the inhibition of CNS QC, but could be due to inhibition of peripheral QC or changes to the ADME of PBD150 in the transgenic mice studied due to long term treatment. Inhibition of QC remains a promising target for the treatment of AD and early detection of AD prior to senile plaque formation. A BBB-permeable QC inhibitor would represent a step forward in the development of a therapeutic agent and could serve as a companion diagnostic when developed as a PET radioligand. To that end, we continue our work to identify a BBB-permeable QC inhibitor. In addition, this work demonstrates that a more detailed understanding of QC inhibition is essential prior to clinical translation.

## Supplementary Material

Refer to Web version on PubMed Central for supplementary material.

## Acknowledgements

We acknowledge the NIH (T32-EB005172), Alzheimer's Association (NIRP-14-305669) and the Michigan Research Community / Undergraduate Research Opportunity Program for financial support, and also thank the Pharmacokinetics Core at the University of Michigan for conducting metabolism studies.

## Notes and references

1. Höfling C, Indrischek H, Höpcke T, Waniek A, Cynis H, Koch B, Schilling S, Morawski M, Demuth H-U, Roßner S, Hartlage-Rübsamen M. *Int. J. Dev. Neurosci.* 2014; 36:64–73. [PubMed: 24886834]
2. Folkers K, Chang J-K, Currie BL, Bowers CY, Weil A, Schally AV. *Biochem. Biophys. Res. Commun.* 1970; 39:110–113. [PubMed: 4986147]
3. (a) Schilling S, Zeitschel U, Hoffmann T, Heiser U, Francke M, Kehlen A, Holzer M, Hutter-Paier B, Prokesch M, Windisch M, Jagla W, Schlenzig D, Lindner C, Rudolph T, Reuter G, Cynis H, Montag D, Demuth H-U, Rossner S. *Nat Med.* 2008; 14:1106–1111. [PubMed: 18836460] (b) Morawski M, Schilling S, Kreuzberger M, Waniek A, Jäger C, Koch B, Cynis H, Kehlen A, Arendt T, Hartlage-Rübsamen M, Demuth H-U, Roßner S. *J. Alzheimer's Dis.* 2014; 39:385–400. [PubMed: 24164736]
4. Nussbaum JM, Schilling S, Cynis H, Silva A, Swanson E, Wangsanut T, Tayler K, Wiltgen B, Hatami A, Ronicke R, Reymann K, Hutter-Paier B, Alexandru A, Jagla W, Graubner S, Glabe CG, Demuth H-U, Bloom GS. *Nature.* 2012; 485:651–655. [PubMed: 22660329]
5. Schilling S, Lauber T, Schaupp M, Manhart S, Scheel E, Böhm G, Demuth H-U. *Biochemistry.* 2006; 45:12393–12399. [PubMed: 17029395]
6. Saido TC, Iwatsubo T, Mann DMA, Shimada H, Ihara Y, Kawashima S. *Neuron.* 14:457–466. [PubMed: 7857653]
7. Piccini A, Russo C, Gliozzi A, Relini A, Vitali A, Borghi R, Giliberto L, Armirotti A, D'Arrigo C, Bachi A, Cattaneo A, Canale C, Torrassa S, Saido TC, Markesbery W, Gambetti P, Tabaton M. *J. Biol. Chem.* 2005; 280:34186–34192. [PubMed: 16103127]
8. Kuo Y-M, Emmerling MR, Woods AS, Cotter RJ, Roher AE. *Biochem. Biophys. Res. Commun.* 1997; 237:188–191. [PubMed: 9266855]
9. Russo C, Saido TC, DeBusk LM, Tabaton M, Gambetti P, Teller JK. *FEBS Lett.* 1997; 409:411–416. [PubMed: 9224700]
10. Harigaya Y, Saido TC, Eckman CB, Prada C-M, Shoji M, Younkin SG. *Biochem. Biophys. Res. Commun.* 2000; 276:422–427. [PubMed: 11027491]
11. Buchholz M, Heiser U, Schilling S, Niestroj AJ, Zunkel K, Demuth H-U. *J. Med. Chem.* 2006; 49:664–677. [PubMed: 16420052]
12. Buchholz M, Hamann A, Aust S, Brandt W, Boehme L, Hoffmann T, Schilling S, Demuth H-U, Heiser U. *J. Med. Chem.* 2009; 52:7069–7080. [PubMed: 19863057]
13. Ramsbeck D, Buchholz M, Koch B, Böhme L, Hoffmann T, Demuth H-U, Heiser U. *J. Med. Chem.* 2013; 56:6613–6625. [PubMed: 23886302]
14. Tran P-T, Hoang V-H, Thorat SA, Kim SE, Ann J, Chang YJ, Nam DW, Song H, Mook-Jung I, Lee J, Lee J. *Bioorg. Med. Chem.* 2013; 21:3821–3830. [PubMed: 23643900]
15. Heiser, U.; Ramsbeck, D.; Demuth, HU. Radiolabelled glutaminyl cyclase inhibitors. CN Patent. CN103561776 A. 2012.
16. For recent examples of methylating thioureas see: Luan Z, Higaki K, Aguilar-Moncayo M, Ninomiya H, Ohno K, García-Moreno MI, Ortiz MC, García Fernández JM, Suzuki Y. *ChemBioChem.* 2009; 10:2780. [PubMed: 19830760] Carley AP, Dixon S, Kilburn JD. *Synthesis.* 2009:2509. Jensen KB, Braxmeier TM, Demarcus M, Frey JG, Kilburn JD. *Chem. Eur. J.* 2002; 8:1300. [PubMed: 11921213] Bruice CT, Dev AP. US Patent. US 6169176 B1. 2001
17. Campopiano, O.; St. Jean, DJ. *Encyclopedia of Reagents for Organic Synthesis.* John Wiley & Sons, Ltd; 2001.
18. Gilissen C, Bormans G, de Groot T, Verbruggen A. *J. Labelled Compd. Radiopharm.* 1998; 41:491.
19. Davidson, AH.; Davies, SJ.; Moffat, DFC. Quinoline and quinoxaline derivatives as inhibitors of kinase enzymatic activity. WO Patent. WO2006117552 A1. 2006.
20. Shao X, Schnau PL, Fawaz M, Scott PJH. *Nucl. Med. Biol.* 2013; 40:109–116. [PubMed: 23123138]

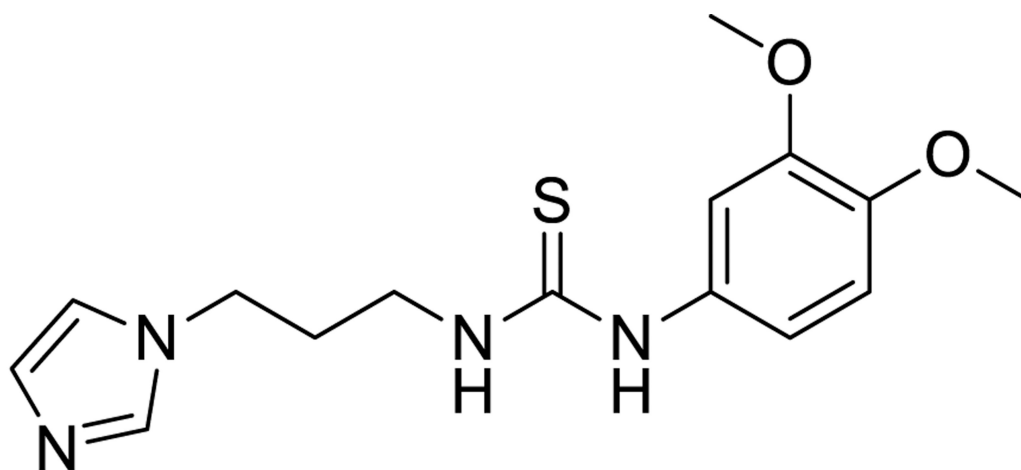
21. Shao X, Carpenter GM, Desmond TJ, Sherman P, Quesada CA, Fawaz M, Brooks AF, Kilbourn MR, Albin RL, Frey KA, Scott PJH. ACS Med. Chem. Lett. 2012; 3:936–941. [PubMed: 24900410]
22. Cole EL, Shao X, Sherman P, Quesada C, Fawaz MV, Desmond TJ, Scott PJH. Nucl. Med. Biol. 2014; 41:507–512. [PubMed: 24768148]

Author Manuscript

Author Manuscript

Author Manuscript

Author Manuscript

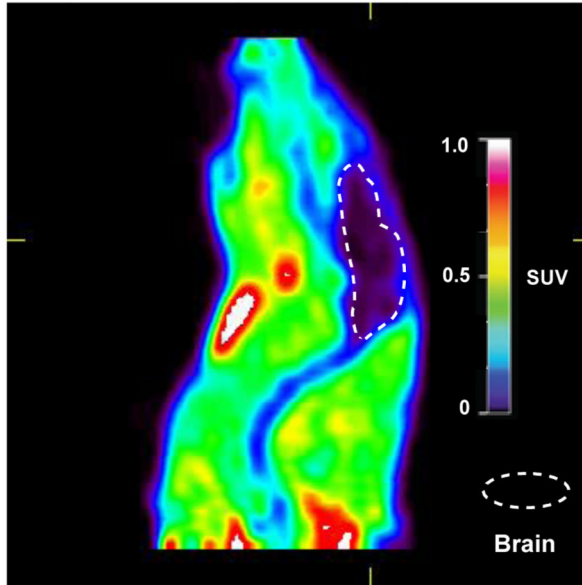


## PBD150

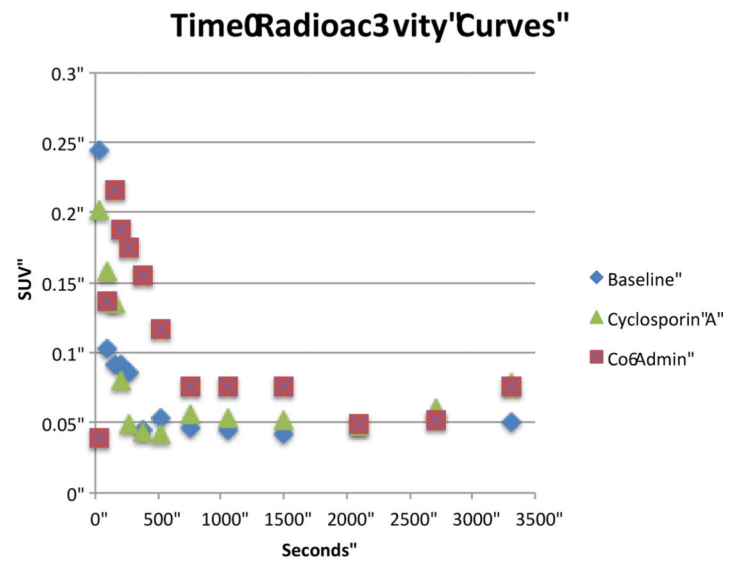
LogBB -1.6,<sup>a</sup> XLogP3 1.5,<sup>b</sup> CLogP 0.92<sup>c</sup>  
K<sub>i</sub> 60 nM (humanQC),<sup>d</sup> K<sub>i</sub> 173 nM (murine QC),<sup>a</sup>

**Figure 1.**  
Structure of PBD150 and properties: a ref,<sup>3</sup> b from Pubchem database, c from ChemBioOffice, d ref.<sup>11</sup>

A''



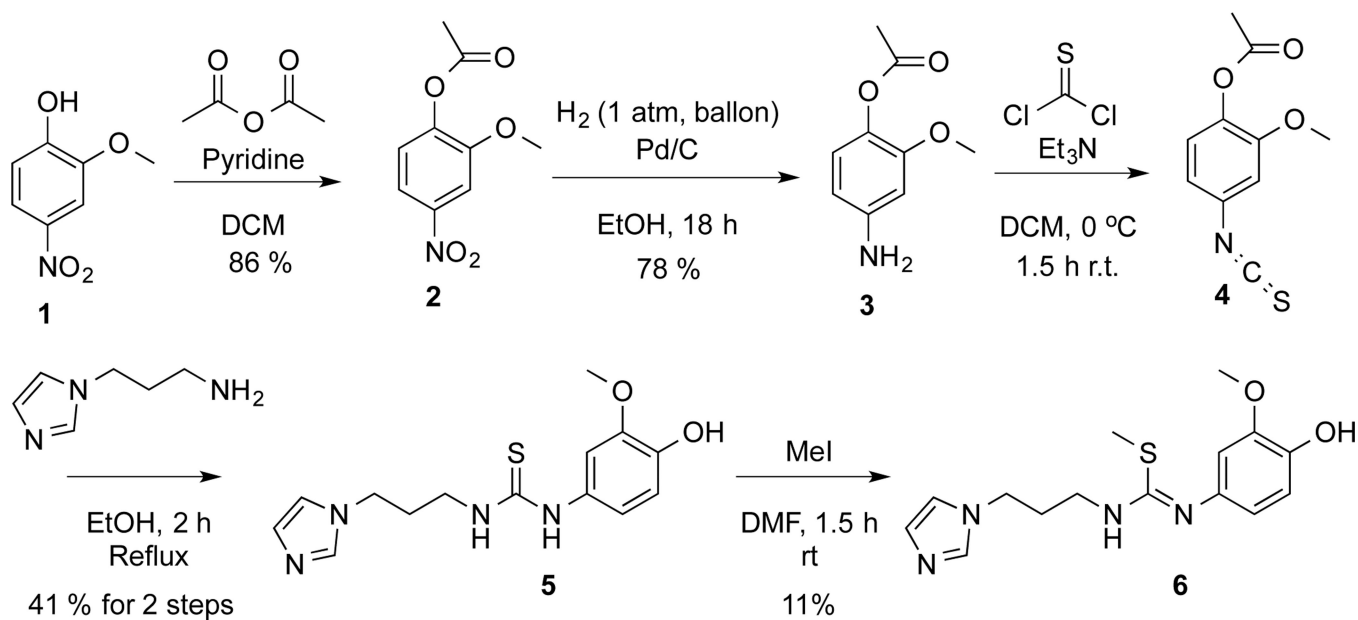
B''



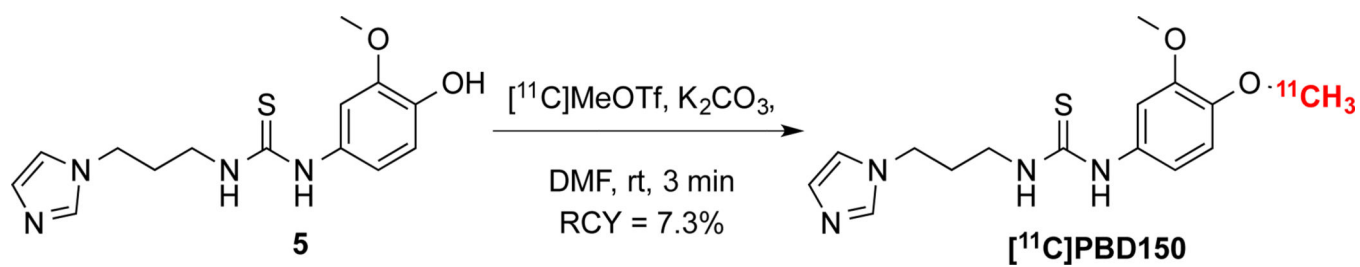
**Figure 2.**

Rodent PET data: A, representative image from [ $^{11}\text{C}$ ]PBD150 co-administration PET scan (summed image 0 – 60 min post-injection of the radiotracer); B, time-radioactivity curves for baseline, cyclosporin A-treated and PBD150 co-administration scans.



**Scheme 1.**

Synthesis of desmethyl precursor of PBD150 **5** and alternate methylation reference standard **6**

**Scheme 2.**

The development of a method to selectively label the phenol over the thiourea was required to produce [ $^{11}\text{C}$ ]PBD150.

Entry	Solvent	Base	Methylating Agent	RCC <sup>a</sup> (PBD150:6)
1	DMF	TBAOH	[ <sup>11</sup> C]MeOTf	0% (0:0) <sup>b</sup>
2	DMF	TBAOH	[ <sup>11</sup> C]MeI	0% (0:0) <sup>b</sup>
3	EtOH Loop	TBAOH	[ <sup>11</sup> C]MeOTf	0% (0:0) <sup>b</sup>
4	DMF	NaH	[ <sup>11</sup> C]MeI	10% (28:72)
5	DMF	NaH	[ <sup>11</sup> C]MeOTf	1% (50:50)
6	3-Pentanone	K <sub>2</sub> CO <sub>3</sub>	[ <sup>11</sup> C]MeOTf	0% (0:0) <sup>c</sup>
7	DMF	K <sub>2</sub> CO <sub>3</sub>	[ <sup>11</sup> C]MeOTf	12% (95:5)
8	DMF	K <sub>2</sub> CO <sub>3</sub>	[ <sup>11</sup> C]MeI	1% (75:25)

<sup>a</sup>% Radiochemical conversions (RCC) represent combined conversion to [<sup>11</sup>C]PBD150 and [<sup>11</sup>C]6. RCC are based upon [<sup>11</sup>C]MeOTf and are uncorrected. Product ratios in parentheses were determined by analytical HPLC;

<sup>b</sup>Precursor decomposed;

<sup>c</sup>Precursor insoluble.